Original Article

Genetic landscape of prognostic value in pancreatic ductal adenocarcinoma microenvironment

Ning Pu[1,2], Qiangda Chen[1], Shanshan Gao[2,3], Gao Liu[4], Yayun Zhu[2,4], Lingdi Yin[2,5], Haijie Hu[2,6], Li Wei[4], Yong Wu[2,7], Shimpei Maeda[2,8], Wenhui Lou[1], Jun Yu[2], Wenchuan Wu[1]

[1]Department of General Surgery, Zhongshan Hospital, Fudan University, Shanghai 200032, China; [2]Department of Surgery and The Pancreatic Cancer Precision Medicine Program, Johns Hopkins University School of Medicine, Baltimore, MD, USA; [3]Department of Interventional Radiology, [4]Department of Liver Surgery and Liver Cancer Institute, Zhongshan Hospital, Fudan University, Shanghai 200032, China; [5]Pancreas Center, The First Affiliated Hospital of Nanjing Medical University, and Pancreas Institute of Nanjing Medical University, Nanjing 210029, China; [6]Department of Biliary Surgery, West China Hospital of Sichuan University, Chengdu 610041, China; [7]Department of General Surgery, The Second Affiliated Hospital of Soochow University, Suzhou 215004, China; [8]Department of Surgery, Tohoku University Graduate School of Medicine, Sendai, Japan

Contributions: (I) Conception and design: N Pu, S Gao, J Yu, W Wu; (II) Administrative support: None; (III) Provision of study materials or patients: None; (IV) Collection and assembly of data: None; (V) Data analysis and interpretation: All authors; (VI) Manuscript writing: All authors; (VII) Final approval of manuscript: All authors.

Correspondence to: Wenchuan Wu, MD, PhD. Department of General Surgery, Zhongshan Hospital, Fudan University, 180 Fenglin Road, Shanghai 200032, China. Email: wu.wenchuan@zs-hospital.sh.cn; Jun Yu, MD, PhD. Department of Surgery, The Sol Goldman Pancreatic Cancer Research Center, The Johns Hopkins University School of Medicine, 600 N. Wolfe Street, Baltimore, MD 21287, USA. Email: jyu41@jhmi.edu.

Background: The prognosis of pancreatic ductal adenocarcinoma (PDAC) remains dismally poor and is widely considered as an intricate genetic disorder. The mutational landscape of PDAC may directly reflect cancer immunogenicity and dictate the extent and phenotype of immune cell infiltration. In adverse, the microenvironment may also effect the gene expression of cancer cells, which is associated with clinical prognosis. Thus, it is crucial to identify genomic alterations in PDAC microenvironment and its impacts on clinical prognosis.

Methods: The gene expression profiles, mutation data and clinical information of 179 pancreatic cancer patients with an initial pathologic diagnosis ranging from 2001 to 2013 were retrieved from The Cancer Genome Atlas (TCGA) database. The MAlignant Tumor tissues using Expression data (ESTIMATE) algorithm for calculating immune scores and stromal scores and Tumor IMmune Estimation Resource (TIMER) resource for cell infiltrations were applied in this study.

Results: The average immune score or stromal score of PDAC subtype was significantly higher than that of other specific subtypes. KRAS mutant cases had significantly lower immune scores (P=0.001) and stromal scores (P=0.007), in concert with lower immune scores in TP53 mutant cases (P=0.030). However, no significant difference was found in SMAD4 and CDKN2A mutations. In the cohort OS/RFS, the infiltration levels of CD8+ T cells, B cells, Macrophages, Neutrophils and DCs in high stromal score group were higher than those in the low score group (all P<0.001), as well as in immune score groups except for Macrophages in the cohort RFS. In the cohort OS/RFS, 317/379 upregulated genes and 9/6 downregulated genes were observed in the high immune score group, while 227/205 upregulated genes and 17/6 downregulated genes in the high stromal score group. With the analysis for prognostic value of DEGs, 82 and 58 DEGs respectively in the high immune and stromal score group were verified to be significantly associated with better OS (P<0.05), while 53 and 17 DEGs respectively with longer RFS (P<0.05). Functional enrichment analysis showed genes of prognostic values were significantly related to immune response.

Conclusions: A list of genes with prognostic value in PDAC microenvironment were obtained from functional enrichment analysis based on immune and stromal scores, which indicates a series of potential auxiliary prognostic biomarkers for PDAC are available. Further research on these genes may be valuable and

helpful to understand the crosstalk between tumor and microenvironment, new immune evasion mechanisms and underlying novel therapeutic targets in an integrated manner.

Introduction

In developed countries, pancreatic cancer turns out to be the fourth leading cause of cancer-related death with a 5-year survival rate of less than 8.0%. In 2019, 56,770 people are predicted to be diagnosed with pancreatic cancer and 45,750 patients will die from the disease in United State (1,2). Although enormous efforts have been made to improve survival of pancreatic cancer patients, the treatment effect is still not obvious. Pancreatic ductal adenocarcinoma (PDAC) is considered as an intricate genetic disorder, therefore, it is crucial to identify genomic alterations in PDAC and its impacts on clinical prognosis.

Nowadays, lots of studies have profiled and analyzed various amounts of PDAC specimens to uncover molecular aberrations at different levels of DNA, RNA, protein and epigenetics by using The Cancer Genome Atlas (TCGA) Research Network (3-5). Recent whole genomes analyses of PDAC have revealed a complex mutational landscape: KRAS, TP53, SMAD4 and CDKN2A are the four most common mutated genes, of which KRAS mutations are near ubiquitous (6). Additionally, mutations of KRAS gene may predict a worse prognosis, which accounts for over 90% of PDAC (7,8).

The tumor microenvironment (TME) is the surroundings where cancer cells exist and absorb nutrients or interact with other ingredients. Besides the cancer cells, the TME is composed of surrounding blood vessels, the extracellular matrix, other non-tumor cells (for example, immune cells, dendritic cells, macrophages and fibroblasts) and also inflammatory mediators (9,10). On one hand, the mutational landscape of cancer cells, a direct reflection of cancer immunogenicity, can dictate the extent and phenotype of immune cell infiltration, and more generally influence the whole TME (11-13). On the other hand, TME also effect the gene expression of cancer cells, which is associated with the clinical prognosis (14-17). Immune and stromal cells, two major components of non-tumor cell populations in

the TME, have been identified as prognostic assessment of tumor (18,19). Then, Yoshihara *et al.* designed an algorithm based on gene expression signatures to estimate the immune and stromal cells, as well as tumor purity, called Estimation of STromal and Immune cells in MAlignant Tumor tissues using Expression data (ESTIMATE) (20). Subsequently, ESTIMATE algorithm has been utilized to prostate cancer (21), cholangiocarcinoma (22), glioblastoma (23), lung cancer (24), breast cancer (25), salivary duct carcinoma (26), colon cancer (27) and many other malignancies, disposing the large data with effect, whereas the immune and/or stromal scores of PDAC in prognostic value has not been sufficiently investigated.

In this study, we focused on the immune and stromal cells that formed the major fraction of non-tumor components of PDAC tissues. By making use of both TCGA PDAC cohorts and immune/stromal scores based on ESTIMATE algorithm, a group of genes related to the microenvironment of PDAC was obtained for predicting prognosis or recurrence, and potential microenvironment associated functions were enriched in high immune/stromal environment.

Methods

Database

Level 3 gene expression profile for pancreatic cancer was downloaded from the TCGA data portal [TCGA pancreatic cancer (PAAD)] (https://xenabrowser.net/datapages/), RNA expression for pancreatic cancer using IlluminaHiSeq_RNASeqV2 (October 13, 2017). Gene mutation details about KRAS, TP53, SMAD4 and CDKN2A, along with data on clinical characteristics such as age, gender, TNM stage, histological type, survival and recurrence was also obtained from TCGA data portal. The downloaded database was applied by the ESTIMATE algorithm for calculating immune scores and stromal scores (https://

bioinformatics.mdanderson.org/estimate/) (20). This study was approved by the Clinical Research Ethic Committee of Zhongshan Hospital, Fudan University (B2014-019).

Tumor IMmune Estimation Resource (TIMER)

The TIMER is a web-based open access resource for systematical analysis of immune infiltrations within various cancers (https://cistrome.shinyapps.io/timer/). All the PDAC cases from TCGA database were estimated for the abundances of six tumor-infiltrating cell populations including CD4^{+} T cells, CD8^{+} T cells, B cells, Macrophages, Neutrophils and Dendritic cells (DCs).

Differentially expressed genes (DEGs) identification

Package "limma" was used for data analysis (28). Fold change (FC) >3 and adj. P<0.05 were set as the cutoffs to identify the DEGs.

Volcano plots and heatmaps for clustering analysis

Volcano plots were generated with all related genes using package "gplots" in PDAC cases with FC >3 and adj. P<0.05. Package "gplots" were also used for generating heatmaps and clustering with DEGs.

Enrichment analysis of DEGs

The Database for Annotation, Visualization and Integrated Discovery (DAVID) (https://david.ncifcrf.gov/) (29) was an open-access tool for functional enrichment analysis of DEGs to identify gene oncology (GO) characteristics including biological processes (BP), molecular functions (MF), and cellular components (CC). Pathway enrichment analysis in reference to Kyoto Encyclopedia of Genes and Genomes (KEGG) pathways was also performed within the DAVID database. False discovery rate (FDR) <0.05 was used as the cut-off.

Protein-protein interaction (PPI) network construction

The PPI network was initially obtained from STRING database (30) and reconstructed via Cytoscape software (31). The minimum required interaction score was set up as 0.400. Further analysis was just applied for individual networks that owned 10 or more nodes, and networks were directly excluded from further study if they have less than 10 nodes. Molecular COmplex Detection (MCODE) was then manipulated to find topology-based clusters to locate regions with a high degree of connectivity.

Analysis

In this study, statistical analyses were performed with statistical software package R (version 3.3.4, http://www.r-project.org/). The Kaplan-Meier survival curves of overall survival (OS) and recurrence free survival (RFS) were generated by Graphpad Prism 7 program, and the Log-rank test for Kaplan-Meier survival curves was conducted to illustrate their relationships to gene mutations or expression levels of DEGs. All P value <0.05 made a significant difference statistically.

Results

Patients characteristics

The gene expression profiles, mutation data and clinical information of 179 pancreatic cancer patients with an initial pathologic diagnosis ranging from 2001 to 2013 were retrieved from the TCGA cohorts. Of them, 99 (55.3%) patients were male and 80 (44.7%) patients were female. Eighty-two patients (45.8%) were less than 65 years old. And 147 (82.1%) patients were pathologically diagnosed as PDAC, while 31 (17.3%) patients were other specific subtypes including neuroendocrine carcinoma, colloid carcinoma, undifferentiated carcinoma and so on. All other clinicopathological characteristics were displayed in *Table S1*. In the total cohort, 172 (96.1%) patients had complete and valid OS data and 152 (84.9%) patients had complete and valid RFS data. Among all PDAC patients, 146 (99.3%) patients had complete and detailed gene mutation data, 141 (95.9%) patients had complete and valid OS data (cohort OS), and 122 (83.0%) patients had complete and valid RFS data (cohort RFS) (*Figure 1*).

Immune scores and stromal scores are significantly associated with PDAC subtype

ESTIMATE algorithm-derived immune scores ranged from –1,559.87 to 3,037.78 (stromal scores: –1,843.32 to 2,179.19, *Figure 2A,B*). The average immune score of PDAC subtype was higher than that of other specific subtypes (*Figure 2A*, P<0.001), as well as stromal score (*Figure 2B*, P=0.007), which indicated that both scores were
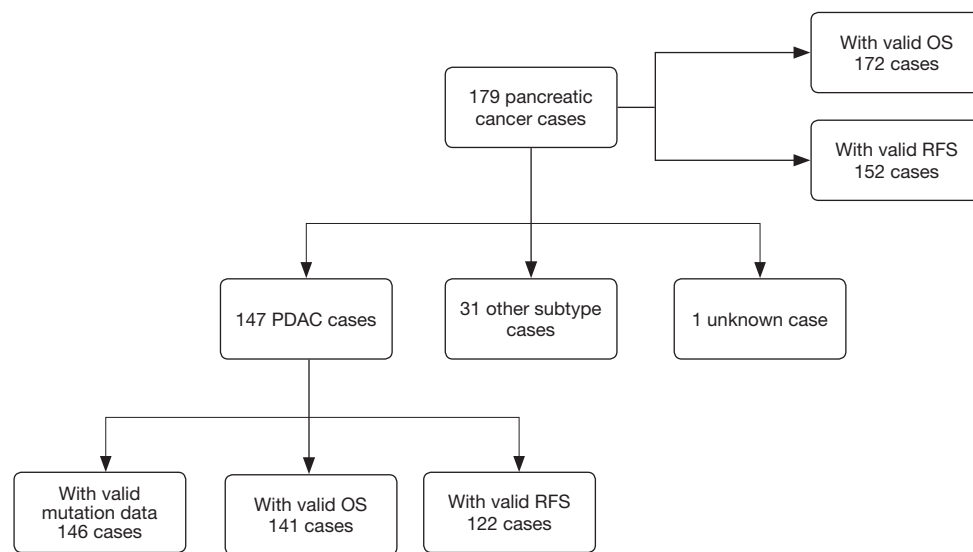
Page 4 of 12

Pu et al. Genetic landscape of prognostic value in PDAC microenvironment

Figure 1 The flow chart of the valid data from TCGA database. TCGA, The Cancer Genome Atlas.

meaningfully correlated with PDAC.

Based on the published four leading mutation gene in PDAC (KRAS, TP53, SMAD4 and CDKN2A), mutations of these genes are prognostic variables for worse survival rates in PDAC. Thus, the distribution of immune/stromal scores according to the status of these four gene mutations in PDAC cases was plotted. The results showed that KRAS mutant cases had significantly lower immune scores (P=0.001) and stromal scores (P=0.007), in concert with lower immune scores in TP53 mutant cases (P=0.030) (*Figure 2C,D,E,F*). However, no significant difference was found in SMAD4 and CDKN2A mutations (*Figure 2G,H,I,J*).

The PDAC cases were parted into high and low score groups to uncover the potential correlation of OS or RFS with immune/stromal scores. Kaplan-Meier survival curves showed that median OS and RFS of cases with the high immune scores was longer than those in the low score group (OS, *Figure 2K*, 596 *vs.* 518 d, P=0.305; RFS, *Figure 2L*, 872 *vs.* 593 d, P=0.241). Consistently, patients with higher stromal scores also had longer median OS and RFS, when compared to those with lower scores (OS, *Figure 2M*, 603 *vs.* 511 d, P=0.427; RFS, *Figure 2N*, 872 *vs.* 620 d, P=0.107), although they were not statistically significant.

Infiltration level of immune cells with immune scores and stromal scores in PDAC

With the estimation of TIMER, the infiltration levels of CD4$^+$ T cells, CD8$^+$ T cells, B cells, Macrophages,

Neutrophils and DCs in PDAC cases were retrieved. In the cohort OS, the infiltration levels of CD4$^+$ T cells, CD8$^+$ T cells, B cells, Macrophages, Neutrophils and DCs in high score group of immune scores were higher than those in the low score group (*Figure 3A*, all P<0.001). However, the infiltration level of CD4$^+$ T cells was significantly lower in the high stromal score group than that in the low stromal score group (*Figure 3B*, all P<0.001). Additionally, in the cohort RFS, the same findings were achieved based on stromal scores (*Figure 3C*, all P<0.001). Concomitantly, the infiltration levels of CD4$^+$ T cells, CD8$^+$ T cells, B cells, Neutrophils and DCs were significantly higher in the high immune score group (all P<0.001) except for macrophages (*Figure 3D*, P=0.113).

Comparison of gene expression profile in PDAC with immune/stromal scores

To find out the correlation of global gene expression profiles with immune/stromal scores, all PDAC cases retrieved from TCGA database were analyzed. Volcano plots in *Figure 4A,B* (heatmaps at http://fp.amegroups.cn/cms/7163e514a5 4a84ea9f6c0cb2c3e9502f/atm.2019.10.91-1.pdf and http:// fp.amegroups.cn/cms/690049836e7ea409972c4702e67c8 84d/atm.2019.10.91-2.pdf) and *Figure S1A,B* (heatmaps at http://fp.amegroups.cn/cms/f09688e3ced2927a8f9ddcac36 fc0b4d/atm.2019.10.91-3.pdf and http://fp.amegroups.cn/ cms/e9c7cee39b6804d69f3d7615402ae928/atm.2019.10.91-4.pdf) displayed distinct gene expression profiles of cases
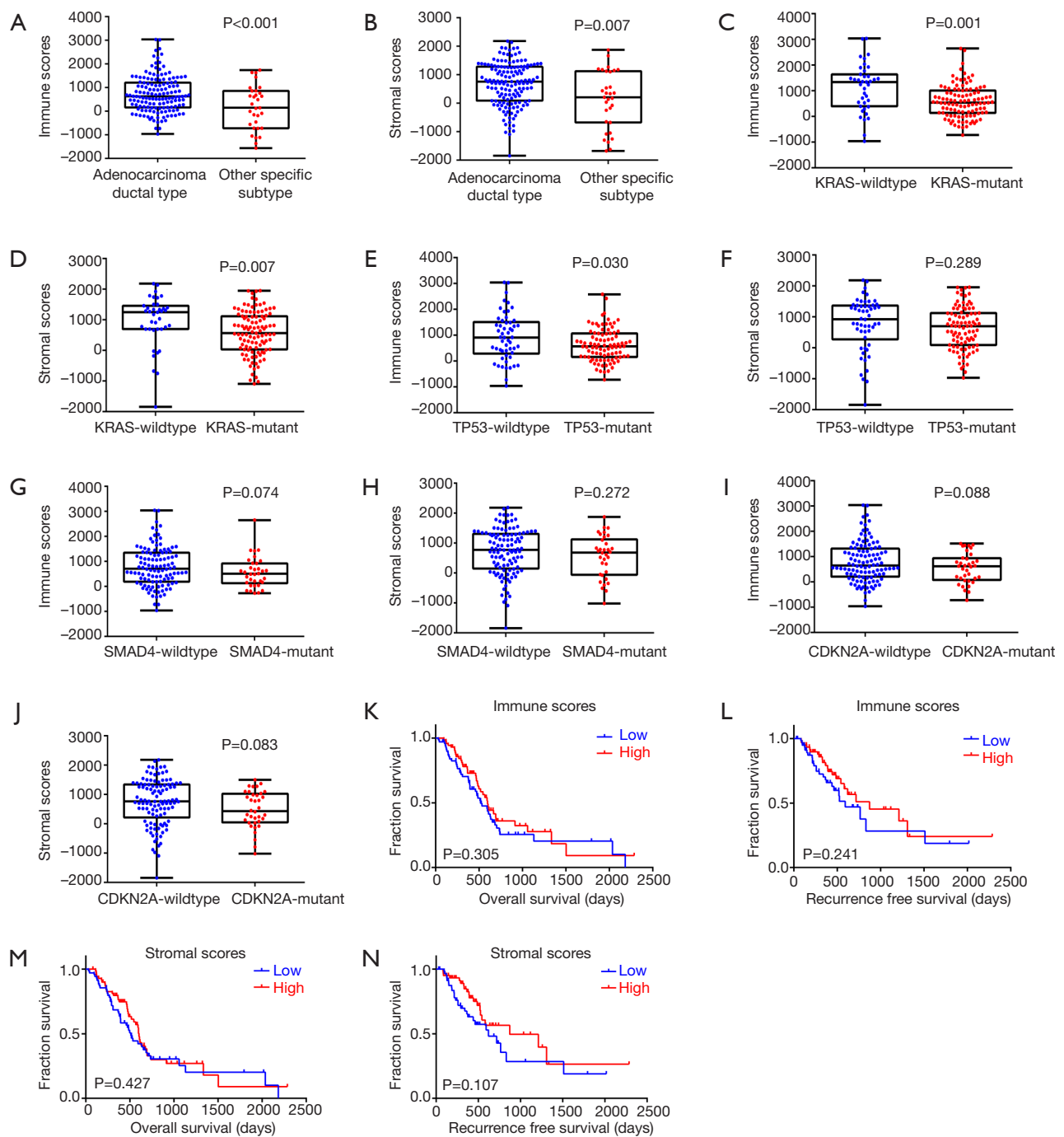
Figure 2 Immune scores and stromal scores are associated with PDAC subtype and their overall survival. Distribution of (A) immune scores and (B) stromal scores of PDAC and other subtypes. Distribution of (C) immune scores and (D) stromal scores for KRAS mutant and KRAS wildtype PDAC cases. Distribution of (E) immune scores and (F) stromal scores for TP53 mutant and TP53 wildtype PDAC cases. Distribution of (G) immune scores and (H) stromal scores for SMAD4 mutant and SMAD4 wildtype PDAC cases. Distribution of (I) immune scores and (J) stromal scores for CDKN2A mutant and CDKN2A wildtype PDAC cases. PDAC cases were divided into two groups based on their immune scores or stromal scores. Kaplan-Meier survival curve of (K) OS and (L) RFS between high and low immune score groups. Kaplan-Meier survival curve of (M) OS and (N) RFS between high and low stromal score groups. PDAC, pancreatic ductal adenocarcinoma; OS, overall survival; RFS, recurrence free survival.
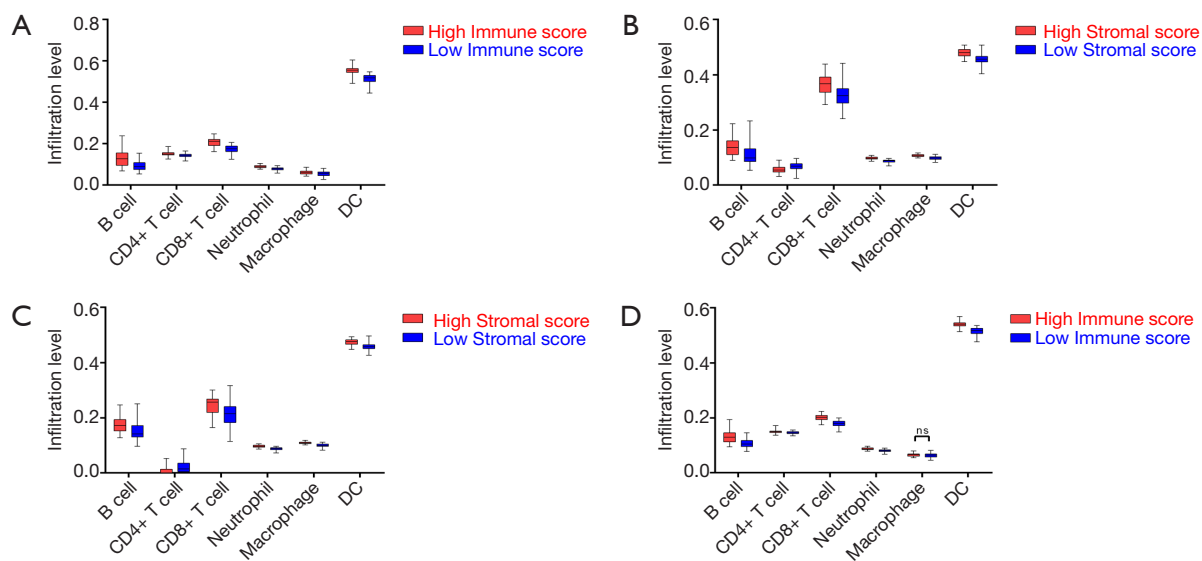
Figure 3 Infiltration level of immune cells with immune scores and stromal scores in PDAC under the estimation of TIMER. In valid OS cohort, the infiltration levels of B cells, CD4+ T cells, CD8+ T cells, Neutrophils, Macrophages, and DCs in PDAC according to (A) immune scores and (B) stromal scores. In valid RFS cohort, the infiltration levels of B cells, CD4+ T cells, CD8+ T cells, Neutrophils, Macrophages, and DCs in PDAC according to (D) immune scores and (C) stromal scores. PDAC, pancreatic ductal adenocarcinoma; OS, overall survival; RFS, recurrence free survival.

between high and low immune/stromal score groups in the cohort OS/RFS. Within the cohort OS, in comparison to low immune score group, 317 upregulated genes and 9 downregulated genes were observed in the high score group (FC >3.0, P<0.05). Likewise, compared to low stromal score group, 227 upregulated genes and 17 downregulated genes were observed in the high score group (FC >3.0, P<0.05). Moreover, Venn diagrams (*Figure 4C,D*) revealed 124 upregulated genes were commonly found in both high score groups, as well as 6 downregulated genes. In the cohort RFS, 379 upregulated genes and 6 downregulated genes were observed in the high score group based on immune scores (FC >3.0, P<0.05), and 205 upregulated genes and 6 downregulated genes were found in the high stromal score group. In addition, Venn diagrams (*Figure S1C,D*) showed that 91 upregulated genes and 2 downregulated genes commonly appeared in both high score groups.

To reveal the underlying functional impacts of the DEGs, functional enrichment analysis of the DEGs were performed in high-immune/stromal score groups. Based on immune scores in the cohort OS, Top GO terms identified included immune, inflammatory and adaptive immune response, integral component of plasma membrane and T cell receptor complex, and receptor and chemokine activity

(*Figure 4E,F,G*), while based on stromal scores, immune and defense response, extracellular region, and carbohydrate and cytokine binding were identified (*Figure 4H,I,J*). According to KEGG pathway analysis, the top one pathway with either immune scores or stromal scores was cytokine-cytokine receptor interaction (*Figure 4K,L*). However, based on immune/stromal scores in the cohort RFS, the top GO terms and KEGG pathways were displayed in *Figure S1E,F,G,H,I,J,K,L*.

Correlation of DEGs expression in OS and RFS

To investigate the potential impacts of individual DEGs on survival, Kaplan-Meier survival curves were plotted and analyzed for the PDAC cohort. Within the total 326 DEGs in the high-immune score group, 82 DEGs were verified to be significantly associated with better OS in log-rank tests (P<0.05), while 58 DEGs were confirmed as better OS predictors in the 244 DEGs in the high-stromal score group (P<0.05, *Table S2*). In addition, among the high-immune score group of 385 DEGs, 53 DEGs were verified to be significantly associated with longer RFS in log-rank tests (P<0.05), and in the high-stromal score group of 221 DEGs, 17 DEGs were associated with longer RFS (P<0.05,
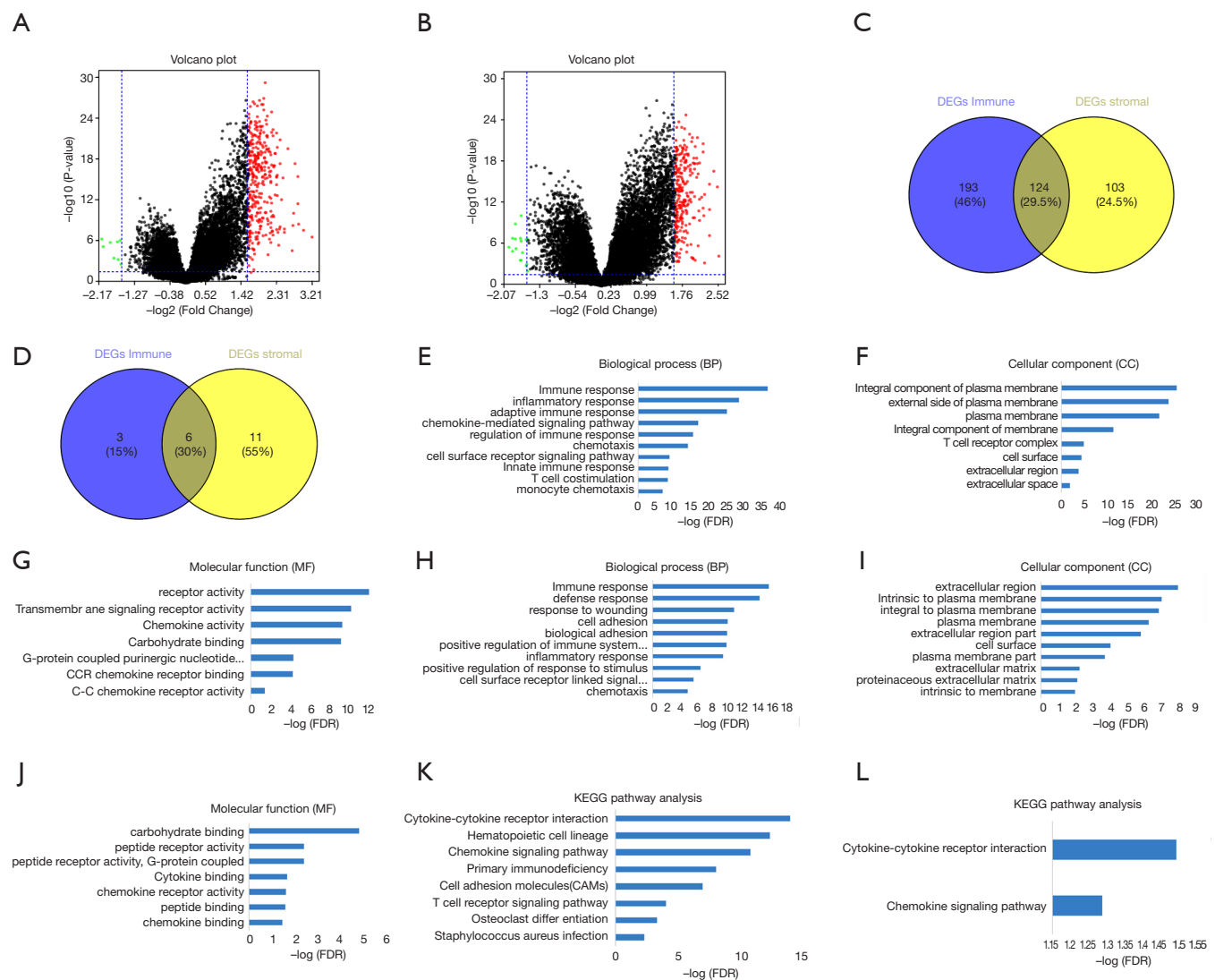
Figure 4 Comparison of gene expression profile with immune scores and stromal scores in valid OS PDAC cohort. (A) Volcano plots of the DEGs of immune scores of top half (high score) *vs.* bottom half (low score). P<0.05, fold change >3. (B) Volcano plots of the DEGs of stromal scores of top half (high score) *vs.* bottom half (low score). P<0.05, fold change >3. Venn diagrams showing the number of commonly (C) upregulated or (D) downregulated DEGs in immune and stromal score groups. (E-J) Top significant GO terms. (K,L) Top significant KEGG pathway analysis. False discovery rate (FDR) of GO and KEGG analysis was acquired from DAVID functional annotation tool. OS, overall survival; PDAC, pancreatic ductal adenocarcinoma; DEGs, differentially expressed genes; GO, gene oncology; KEGG, Kyoto Encyclopedia of Genes and Genomes; DAVID, the Database for Annotation, Visualization and Integrated Discovery.

Table S3).

PPI of genes with prognostic value

PPI networks with the STRING and Cytoscape tool were administrated to better illustrate the interactions among the identified DEGs related to OS/RFS in high immune/stromal score groups. The network consisted of 8 modules including 146 nodes and 473 edges. The top two most significant modules were selected for further analysis (*Figure 5*). For the purpose of convenience of recognition, specific names were given to these two modules—CNR2 and CCL22
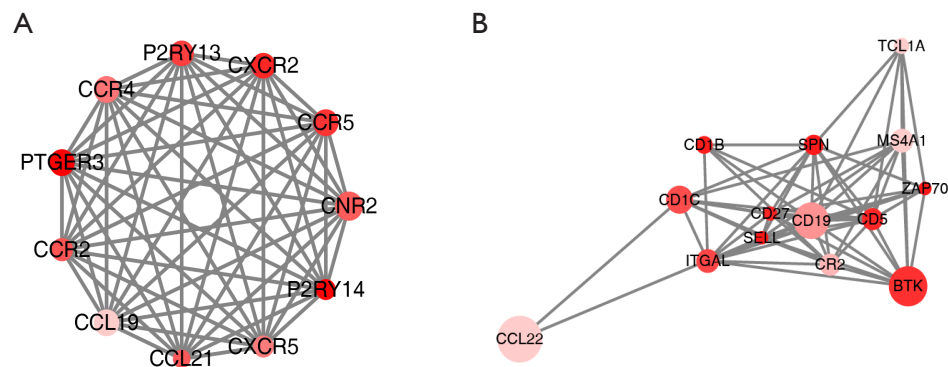
Figure 5 Top 2 protein-protein interaction (PPI) networks of CNR2 and CCL22 modules. The color of a node in the PPI network reflects the log (FC) value of the Z score of gene expression, and the size of node indicates the number of interacting proteins with the designated protein.

modules, respectively. In the CNR2 module (*Figure 5A*), the remarkable 11 nodes involved in 55 edges formed in the network. CNR2, CCR5, CXCR2, CCR4, P2RY13, PTGER3, and CCL19 were typically presented in this network, as they had the highest degree of connectivity with other members of the module. Meanwhile, in the CCL22 module (*Figure 5B*), CCL22, BTK, CD19, and CD1C had higher degree values.

Functional enrichment analysis of genes with prognostic value

Functional enrichment analysis of these genes indicated robust relationship with immune response, which was consistent with PPI network analysis. In the enrichment analysis, a total of 9 GO terms of BP, 6 of CC and 2 of MF were found to be significant (FDR, or FDR <0.05, -log FDR >1.301). Top GO terms included immune and adaptive immune response (*Figure 6A*), plasma and integral of plasma membrane (*Figure 6B*), and chemokine receptor activity (*Figure 6C*). What's more, altered transcriptional output in the pathways yielded from the KEGG analysis (*Figure 6D*) were associated with immune response.

Discussion

In this study, we attempted to take advantage of samples in the TCGA database to obtain a list of genes that related to the PDAC microenvironment, which supported to predict prognosis or recurrence. Based on immune/stromal scores from the ESTIMATE algorithm, we found that both

scores were higher in PDAC subtype. When considering to frequent gene mutation related to PDAC, significant increasing scores were found in KRAS and TP53 mutation. Although there was no statistical difference in high *vs.* low immune/stromal score groups, cases with higher immune/stromal scores may actually obtain a longer OS or RFS. As recently reported, higher immune cell score was validated to be associated with better prognosis of resected PDAC patients (32,33). So that we utilized TIMER, an open-access web server for comprehensive analysis of tumor-infiltrating immune cells, to characterize the landscape of immune infiltrations, which was crucial for the investigation and validation of immune scores and looked for the distribution of each immune components (34). Intriguingly, just CD4+ T cells showed an adverse trend in high *vs.* low immune/stromal score groups.

Then, by comparing global gene expression within the high *vs.* low immune (stromal) scores, 326 DEGs for cohort OS and 485 DEGs for cohort RFS were found to be involved in TME, totally enriching in immune, inflammatory and adaptive immune response, T cell receptor complex, and cytokine and chemokine activity, which further validated the essential role of immune regulations in the formation of PDAC microenvironment (35-37).

Next, OS and RFS of these DEGs were analyzed to identify a list of genes were associated with prognosis and recurrence in PDAC patients in terms of immune/stromal scores. Accordingly, 8 PPI network modules were depicted through STRING and Cytoscape tool, and all of which showed strong associations with immune response.
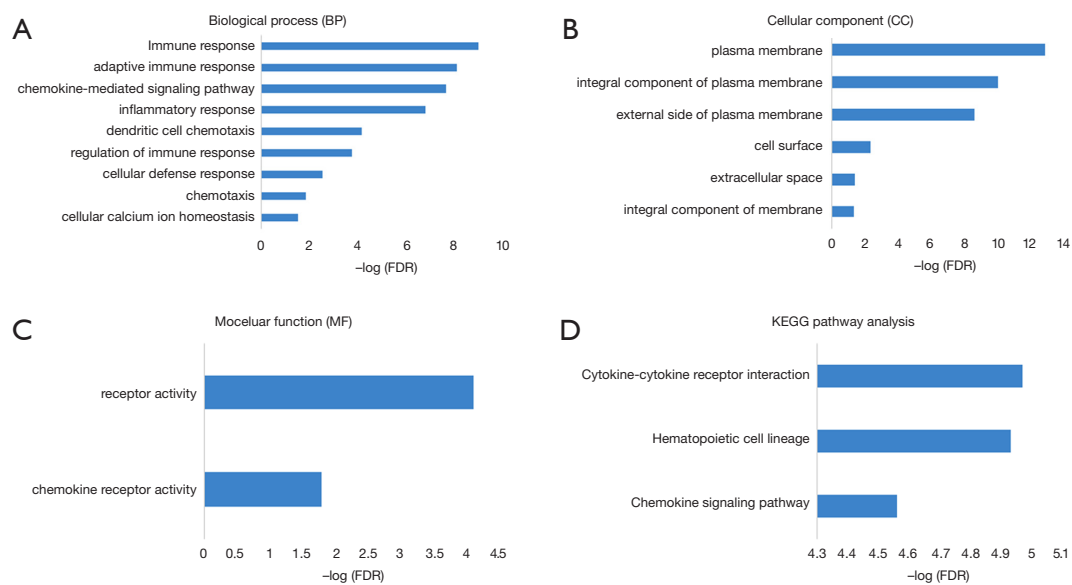
Figure 6 GO term and KEGG pathway analysis for DEGs significantly associated with prognosis. Top pathways with FDR <0.05, –log FDR >1.301 are shown: (A) biological process, (B) cellular component, (C) molecular function, and (D) KEGG pathway. GO, gene oncology; KEGG, Kyoto Encyclopedia of Genes and Genomes; DEGs, differentially expressed genes; FDR, false discovery rate.

From the PPI networks, CNR2 and CCL22 are highly interconnected nodes. CNR2 encodes the Cnr2 receptor, which is highly expressed in T and B lymphocytes, dendritic cells, natural killer cells, monocyte/macrophages, and neutrophils (38,39). Many studies verified CNR2 expressed highly in tumor-associated macrophages or various cancer cells and its expression was proved to be correlated with poor prognosis (40-43). However, CNR2 was also proved as an efficient prognostic regulator for some specific cancers in several researches, which had not previously been linked with PDAC prognosis (44-46). In our study, CNR2 was significantly proved to be associated with a better prognosis for PDAC patients. Likewise, CCL22, known as macrophage-derived chemokine, abundantly expressed in many malignancies was correlated with migration of regulatory T cells (47,48). It has been widely reported for its role in tumor-associated immunosuppression and could further predict reduced survival (47-50). It was strange that CCL22 expression in microenvironment displayed a positive role in survival of PDAC patients within our study, which may potentially facilitate other immune components except for regulatory T cells. However, Nakanishi *et al.* (51) previously reported that macrophage-derived CCL22 in human lung cancer was significantly correlated with lower risk of recurrence after tumor resection and longer RFS, which was consistent with our findings.

The study of tumor gene expression profiles contributes to the identification of molecular subtypes and the establishment of predictive prognostic models, enriching our understanding of the molecular pathways of tumorigenesis (6). In addition, in our previous research, we found the tumor infiltrating CD8+ T cells in PDAC were significantly associated with survival, while tumor infiltrating Tregs had the adverse role. Also, TGF-beta blockade combined with depletion of Treg or DC vaccine administration were verified to successfully inhibit PDAC growth (2,52). All our previous results showed PDAC microenvironment had a giant impact on tumor progression. Concomitantly, pancreatic cancer cell-intrinsic PD-1 was also identified and proved its role in tumor progression (53). Current progresses in cancer immunotherapy and the reduced cost of high-throughput techniques have led to extensive investigations of tumor immune cell communications by means of genomic tools. Thus, through our mining the PDAC microenvironment related genes with valuable prognostic roles, some novel microenvironment related gene panel may be established for survival or recurrence prediction. However, owing to the heterogeneity of the tumor genomes and the plasticity of the host immune system, the communication between tumor cells and immune infiltrations remains a testing research topic and further validations are preferred (54).

Page 10 of 12

Pu et al. Genetic landscape of prognostic value in PDAC microenvironment

However, there were still some limitations in this study. First, all the data are retrieved from the public database and external validations will be required to verify our findings. Second, the significance of up- and down-regulated genes may not be the answers to what is really driving the aggressive biology of pancreatic cancer, so further mechanistic study of these genes are encouraged.

In conclusion, we have extracted a list of genes with prognostic value in PDAC microenvironment from functional enrichment analysis of TCGA database based on immune and stromal scores in our study. These genes can be useful to predict the prognosis of PDAC patients and show their potentials to be auxiliary prognostic biomarkers for PDAC. Additionally, further research on these genes may be valuable and helpful to understand the crosstalk between tumor and microenvironment, new immune evasion mechanisms and underlying novel therapeutic targets in an integrated manner.

Acknowledgments

Footnote

Conflicts of Interest: The authors have no conflicts of interest to declare.

Ethical Statement: The authors are accountable for all aspects of the work in ensuring that questions related to the accuracy or integrity of any part of the work are appropriately investigated and resolved. This study was approved by the Clinical Research Ethic Committee of Zhongshan Hospital, Fudan University (B2014-019).

References

1. Siegel RL, Miller KD, Jemal A. Cancer statistics, 2019. CA Cancer J Clin 2019;69:7-34.
2. Pu N, Zhao G, Yin H, et al. CD25 and TGF-beta blockade based on predictive integrated immune ratio inhibits tumor growth in pancreatic cancer. J Transl Med 2018;16:294.
3. Ho J, Li X, Zhang L, et al. Translational genomics in pancreatic ductal adenocarcinoma: A review with re-analysis of TCGA dataset. Semin Cancer Biol 2019;55:70-7.
4. Yan Y, Gao R, Trinh TLP, et al. Immunodeficiency in Pancreatic Adenocarcinoma with Diabetes Revealed by Comparative Genomics. Clin Cancer Res 2017;23:6363-73.
5. Cancer Genome Atlas Research Network. Electronic address aadhe, Cancer Genome Atlas Research N. Integrated Genomic Characterization of Pancreatic Ductal Adenocarcinoma. Cancer Cell 2017;32:185-203.e13.
6. Waddell N, Pajic M, Patch AM, et al. Whole genomes redefine the mutational landscape of pancreatic cancer. Nature 2015;518:495-501.
7. Bournet B, Muscari F, Buscail C, et al. KRAS G12D Mutation Subtype Is A Prognostic Factor for Advanced Pancreatic Adenocarcinoma. Clin Transl Gastroenterol 2016;7:e157.
8. Kwon MJ, Jeon JY, Park HR, et al. Low frequency of KRAS mutation in pancreatic ductal adenocarcinomas in Korean patients and its prognostic value. Pancreas 2015;44:484-92.
9. Junttila MR, de Sauvage FJ. Influence of tumour microenvironment heterogeneity on therapeutic response. Nature 2013;501:346-54.
10. Hanahan D, Weinberg RA. Hallmarks of Cancer: The Next Generation. Cell 2011;144:646-74.
11. Petitprez F, Vano YA, Becht E, et al. Transcriptomic analysis of the tumor microenvironment to guide prognosis and immunotherapies. Cancer Immunol Immunother 2018;67:981-8.
12. Li J, Byrne KT, Yan F, et al. Tumor Cell-Intrinsic Factors Underlie Heterogeneity of Immune Cell Infiltration and Response to Immunotherapy. Immunity 2018;49:178-93.e7.
13. Binnewies M, Roberts EW, Kersten K, et al. Understanding the tumor immune microenvironment (TIME) for effective therapy. Nat Med 2018;24:541-50.
14. Maley CC, Aktipis A, Graham TA, et al. Classifying the evolutionary and ecological features of neoplasms. Nat Rev Cancer 2017;17:605-19.
15. Herrera M, Islam ABMMK, Herrera A, et al. Functional Heterogeneity of Cancer-Associated Fibroblasts from Human Colon Tumors Shows Specific Prognostic Gene Expression Signature. Clinical Cancer Research 2013;19:5914-26.
16. Cooper LA, Gutman DA, Chisolm C, et al. The tumor microenvironment strongly impacts master transcriptional

regulators and gene expression class of glioblastoma. Am J Pathol 2012;180:2108-19.

17. Artacho-Cordón A, Artacho-Cordon F, Rios-Arrabal S, et al. Tumor microenvironment and breast cancer progression: a complex scenario. Cancer Biol Ther 2012;13:14-24.

18. Efstathiou JA, Mouw KW, Gibb EA, et al. Impact of Immune and Stromal Infiltration on Outcomes Following Bladder-Sparing Trimodality Therapy for Muscle-Invasive Bladder Cancer. Eur Urol 2019;76:59-68.

19. Mahajan UM, Langhoff E, Goni E, et al. Immune Cell and Stromal Signature Associated With Progression-Free Survival of Patients With Resected Pancreatic Ductal Adenocarcinoma. Gastroenterology 2018;155:1625-39.e2.

20. Yoshihara K, Shahmoradgoli M, Martinez E, et al. Inferring tumour purity and stromal and immune cell admixture from expression data. Nat Commun 2013;4:2612.

21. Fraser M, Sabelnykova VY, Yamaguchi TN, et al. Genomic hallmarks of localized, non-indolent prostate cancer. Nature 2017;541:359-64.

22. Jusakul A, Cutcutache I, Yong CH, et al. Whole-Genome and Epigenomic Landscapes of Etiologically Distinct Subtypes of Cholangiocarcinoma. Cancer Discov 2017;7:1116-35.

23. Jia D, Li S, Li D, et al. Mining TCGA database for genes of prognostic value in glioblastoma microenvironment. Aging (Albany NY) 2018;10:592-605.

24. Karlsson A, Jonsson M, Lauss M, et al. Genome-wide DNA methylation analysis of lung carcinoma reveals one neuroendocrine and four adenocarcinoma epitypes associated with patient outcome. Clin Cancer Res 2014;20:6127-40.

25. Abba MC, Gong T, Lu Y, et al. A Molecular Portrait of High-Grade Ductal Carcinoma In Situ. Cancer Res 2015;75:3980-90.

26. Dalin MG, Desrichard A, Katabi N, et al. Comprehensive Molecular Characterization of Salivary Duct Carcinoma Reveals Actionable Targets and Similarity to Apocrine Breast Cancer. Clin Cancer Res 2016;22:4623-33.

27. Alonso MH, Ausso S, Lopez-Doriga A, et al. Comprehensive analysis of copy number aberrations in microsatellite stable colon cancer in view of stromal component. Br J Cancer 2017;117:421-31.

28. Ritchie ME, Phipson B, Wu D, et al. limma powers differential expression analyses for RNA-sequencing and microarray studies. Nucleic Acids Res 2015;43:e47.

29. Huang W, Sherman BT, Lempicki RA. Systematic and integrative analysis of large gene lists using DAVID bioinformatics resources. Nat Protoc 2009;4:44-57.

30. Szklarczyk D, Franceschini A, Wyder S, et al. STRING v10: protein-protein interaction networks, integrated over the tree of life. Nucleic Acids Res 2015;43:D447-52.

31. Shannon P, Markiel A, Ozier O, et al. Cytoscape: A software environment for integrated models of biomolecular interaction networks. Genome Res 2003;13:2498-504.

32. Tahkola K, Leppanen J, Ahtiainen M, et al. Immune cell score in pancreatic cancer-comparison of hotspot and whole-section techniques. Virchows Arch 2019.

33. Tahkola K, Mecklin JP, Wirta EV, et al. High immune cell score predicts improved survival in pancreatic cancer. Virchows Arch 2018;472:653-65.

34. Li T, Fan J, Wang B, et al. TIMER: A Web Server for Comprehensive Analysis of Tumor-Infiltrating Immune Cells. Cancer Res 2017;77:e108-10.

35. Sherman MH, Yu RT, Tseng TW, et al. Stromal cues regulate the pancreatic cancer epigenome and metabolome. Proc Natl Acad Sci U S A 2017;114:1129-34.

36. Chang JH, Jiang Y, Pillarisetty VG. Role of immune cells in pancreatic cancer from bench to clinical application: An updated review. Medicine (Baltimore) 2016;95:e5541.

37. Feig C, Gopinathan A, Neesse A, et al. The pancreas cancer microenvironment. Clin Cancer Res 2012;18:4266-76.

38. Rieder SA, Chauhan A, Singh U, et al. Cannabinoid-induced apoptosis in immune cells as a pathway to immunosuppression. Immunobiology 2010;215:598-605.

39. Pandey R, Mousawy K, Nagarkatti M, et al. Endocannabinoids and immune regulation. Pharmacol Res 2009;60:85-92.

40. Wang J, Xu YZ, Zhu LS, et al. Cannabinoid receptor 2 as a novel target for promotion of renal cell carcinoma prognosis and progression. J Cancer Res Clin Oncol 2018;144:39-52.

41. Pérez-Gómez E, Andradas C, Blasco-Benito S, et al. Role of cannabinoid receptor CB2 in HER2 pro-oncogenic signaling in breast cancer. J Natl Cancer Inst 2015;107:djv077.

42. Xiang W, Shi R, Kang X, et al. Monoacylglycerol lipase regulates cannabinoid receptor 2-dependent macrophage activation and cancer progression. Nat Commun 2018;9:2574.

43. Martínez-Martínez E, Martin-Ruiz A, Martin P, et al. CB2 cannabinoid receptor activation promotes colon cancer progression via AKT/GSK3beta signaling pathway.

Oncotarget 2016;7:68781-91.

44. Elbaz M, Ahirwar D, Ravi J, et al. Novel role of cannabinoid receptor 2 in inhibiting EGF/EGFR and IGF-I/IGF-IR pathways in breast cancer. Oncotarget 2017;8:29668-78.

45. Bettiga A, Aureli M, Colciago G, et al. Bladder cancer cell growth and motility implicate cannabinoid 2 receptor-mediated modifications of sphingolipids metabolism. Sci Rep 2017;7:42157.

46. Ravi J, Elbaz M, Wani NA, et al. Cannabinoid receptor-2 agonist inhibits macrophage induced EMT in non-small cell lung cancer by downregulation of EGFR pathway. Mol Carcinog 2016;55:2063-76.

47. Gobert M, Treilleux I, Bendriss-Vermare N, et al. Regulatory T Cells Recruited through CCL22/CCR4 Are Selectively Activated in Lymphoid Infiltrates Surrounding Primary Breast Tumors and Lead to an Adverse Clinical Outcome. Cancer Res 2009;69:2000-9.

48. Curiel TJ, Coukos G, Zou L, et al. Specific recruitment of regulatory T cells in ovarian carcinoma fosters immune privilege and predicts reduced survival. Nat Med 2004;10:942-9.

49. Wu S, He H, Liu H, et al. C-C motif chemokine 22 predicts postoperative prognosis and adjuvant chemotherapeutic benefits in patients with stage II/III gastric cancer. Oncoimmunology 2018;7:e1433517.

50. Wiedemann GM, Knott MM, Vetter VK, et al. Cancer cell-derived IL-1alpha induces CCL22 and the recruitment of regulatory T cells. Oncoimmunology 2016;5:e1175794.

51. Nakanishi T, Imaizumi K, Hasegawa Y, et al. Expression of macrophage-derived chemokine (MDC)/CCL22 in human lung cancer. Cancer Immunol Immunother 2006;55:1320-9.

52. Pu N, Zhao G, Gao S, et al. Neutralizing TGF-beta promotes anti-tumor immunity of dendritic cells against pancreatic cancer by regulating T lymphocytes. Cent Eur J Immunol 2018;43:123-31.

53. Pu N, Gao S, Yin H, et al. Cell-intrinsic PD-1 promotes proliferation in pancreatic cancer by targeting CYR61/CTGF via the hippo pathway. Cancer Lett 2019;460:42-53.

54. Hackl H, Charoentong P, Finotello F, et al. Computational genomics tools for dissecting tumour-immune cell interactions. Nat Rev Genet 2016;17:441-58.

Table S1 The clinicopathological stigma of the PAAD TCGA data

| Variables	No. of patients (n, %), total n=179
Age	
<65	82 (45.8)
≥65	97 (54.2)
Mass location	
Head	139 (77.7)
Body	14 (7.8)
Tail	15 (8.4)
Others	11 (6.1)
Gender	
Female	80 (44.7)
Male	99 (55.3)
Grade	
G1	31 (17.3)
G2	96 (53.6)
G3	48 (26.8)
G4	2 (1.1)
GX	2 (1.1)
AJCC 7th staging	
I	21 (11.7)
II	147 (82.1)
III	4 (2.2)
IV	5 (2.8)
Unknown	2 (1.1)
T staging	
T1	7 (3.9)
T2	24 (13.4)
T3	143 (79.9)
T4	3 (1.7)
TX	2 (1.1)
N staging	
N0	51 (28.5)
N1	124 (69.3)
NX	4 (2.2)
Margin	
R0	117 (65.4)
R1	53 (29.6)
R2	5 (2.8)
RX	4 (2.2)
Histological type	
Adenocarcinoma ductal type	147 (82.1)
Colloid (mucinous non-cystic) carcinoma	4 (2.2)
Neuroendocrine carcinoma	8 (4.5)
Other subtypes	19 (10.6)
Unknown	1 (0.6)
KRAS mutation	
Yes	124 (69.3)
No	54 (30.2)
Unknown	1 (0.6)
TP53 mutation	
Yes	106 (59.2)
No	72 (40.2)
Unknown	1 (0.6)
SMAD4 mutation	
Yes	37 (20.7)
No	141 (78.8)
Unknown	1 (0.6)
CDKN2A mutation	
Yes	41 (22.9)
No	137 (76.5)
Unknown	1 (0.6)

TCGA, The Cancer Genome Atlas.
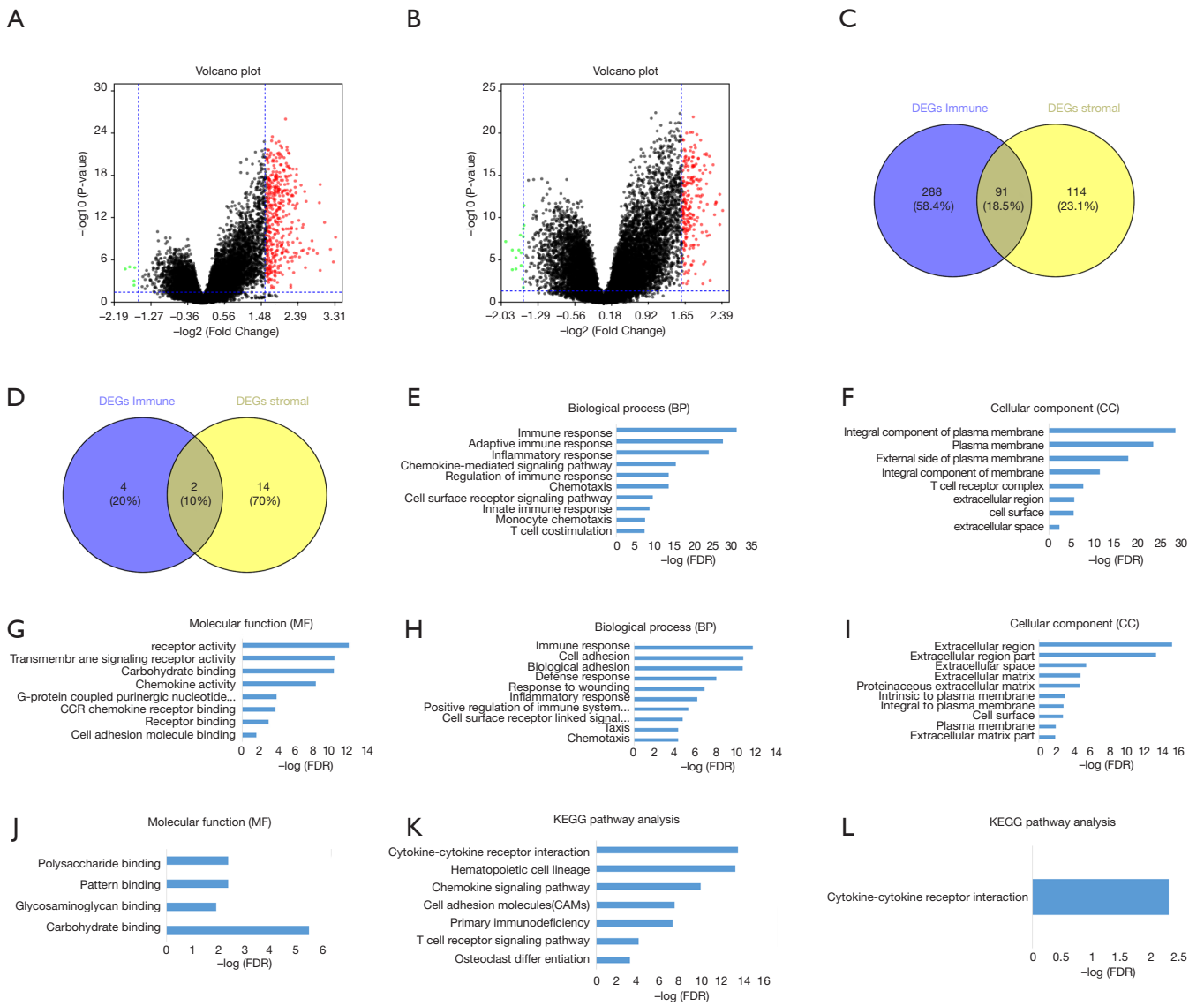
Figure S1 Comparison of gene expression profile with immune scores and stromal scores in valid RFS PDAC cohort. (A) Volcano plots of the DEGs of immune scores of top half (high score) *vs.* bottom half (low score). P<0.05, fold change >3. (B) Volcano plots of the DEGs of stromal scores of top half (high score) *vs.* bottom half (low score). P<0.05, fold change >3. Venn diagrams showing the number of commonly (C) upregulated or (D) downregulated DEGs in immune and stromal score groups. (E-J) Top significant GO terms. (K,L) Top significant KEGG pathway analysis. False discovery rate (FDR) of GO and KEGG analysis was acquired from DAVID functional annotation tool. RFS, recurrence free survival; PDAC, pancreatic ductal adenocarcinoma; DEGs, differentially expressed genes; GO, gene oncology; KEGG, Kyoto Encyclopedia of Genes and Genomes; DAVID, the Database for Annotation, Visualization and Integrated Discovery.

Table S2 Differentially expression genes (DEGs) with significant OS predictor in the high immune/stromal scores group

Gene	OS	
	P value	HR
Immune score group		
CXCR2P1	0.047	0.992
CILP	0.025	0.950
SLCO2B1	0.01	0.889
CD226	0.037	0.907
NLRC4	0.032	0.886
TCL1A	0.045	0.949
PAX5	0.048	0.932
CXCR2	0.04	0.917
TARP	0.037	0.890
IGF1	0.032	0.922
SCN7A	0.042	0.926
CCR5	0.013	0.885
CNR2	0.026	0.912
GPR65	0.04	0.859
LILRB1	0.032	0.874
LY86	0.006	0.876
FCER2	0.016	0.926
CTSG	<0.001	0.911
FCRLA	0.019	0.919
DPEP2	0.032	0.869
CR2	0.02	0.946
TFEC	0.041	0.869
SELL	0.023	0.865
KCNA3	0.025	0.874
CCR4	0.039	0.892
MAL	0.025	0.871
ABCA8	0.018	0.882
LILRA4	0.031	0.885
KLHL6	0.013	0.846
CD19	0.005	0.912
P2RY8	0.043	0.842
SNX20	0.01	0.834
LCP1	0.016	0.841
CLEC17A	0.025	0.881
IKZF1	0.025	0.853
CCL22	0.011	0.865
CD36	0.019	0.883
FCRL3	0.023	0.890
BIN2	0.044	0.822
SLC24A4	0.013	0.834
ITGAL	0.016	0.851
TRAF3IP3	0.034	0.836
CCL21	0.012	0.893
WDFY4	0.007	0.867
ITK	0.032	0.863
PRKCB	0.048	0.867
CD27	0.039	0.847
ANK2	0.006	0.839
WAS	0.028	0.810
CD200R1	0.018	0.829
TNFRSF13B	0.005	0.877
ADIPOQ	0.03	0.930
PI16	0.029	0.907
CHRDL1	0.04	0.885
MS4A1	0.017	0.918
CD5	0.03	0.832
P2RY14	0.016	0.830
PLA2G2D	0.019	0.890
IGJ	0.047	0.889
TNNT1	0.006	1.103
PKHD1L1	0.018	0.848
MAP4K1	0.018	0.840
SPN	0.001	0.822
GIMAP7	0.008	0.808
RELN	0.005	0.876
IL10RA	0.041	0.782
ABCD2	0.018	0.833
TUSC5	0.03	0.883
ZNF831	0.005	0.859
CCL19	0.024	0.895
CCL23	0.026	0.846
EMR3	0.04	0.837
CELF2	<0.001	0.800
ZAP70	0.022	0.813
KIAA0748	0.016	0.810
CFP	0.01	0.784
SCARA5	0.001	0.871
PLA2G2A	0.01	0.890
C5orf20	0.042	0.798
C16orf89	0.006	0.817
BEND4	0.017	0.776
DARC	0.029	0.841
RASGRP2	0.004	0.769
Stromal score group		
FBN1	0.024	0.968
PPFIA2	0.028	0.964
KLHL4	0.031	0.956
SEMA3D	0.039	0.953
ADAM22	0.03	0.936
CILP	0.025	0.950
STON1-CTF2A1L	0.024	0.945
ITGA9	0.024	0.928
GPNMB	0.044	0.910
PTGER3	0.004	0.903
EBF2	0.039	0.926
PIK3CG	0.039	0.912
SPON1	0.01	0.893
SLCO2B1	0.01	0.889
CD226	0.037	0.907
TCL1A	0.045	0.949
ADAM23	0.025	0.907
CXCR2	0.04	0.917
ABCC9	0.045	0.885
IGF1	0.032	0.922
SCN7A	0.042	0.926
CCR5	0.013	0.885
NEXN	0.035	0.865
NRXN1	0.037	0.900
CTSG	<0.001	0.911
FCRLA	0.019	0.919
CR2	0.02	0.946
SFRP4	0.039	0.879
TFEC	0.041	0.869
KCNK2	0.042	0.875
NLGN4X	0.032	0.857
SLIT3	0.035	0.861
KCNA3	0.025	0.874
CCR4	0.039	0.892
ABCA8	0.018	0.882
KLHL6	0.013	0.846
CD19	0.005	0.912
IKZF1	0.025	0.853
FCRL3	0.023	0.890
SFRP1	0.033	0.887
WDFY4	0.007	0.867
ITK	0.032	0.863
PRKCB	0.048	0.867
ANK2	0.006	0.837
ADIPOQ	0.03	0.930
CHRDL1	0.04	0.885
MS4A2	0.033	0.821
MS4A1	0.017	0.918
PLA2G2D	0.019	0.890
IGJ	0.047	0.890
GHR	0.028	0.801
TNNT1	0.006	1.103
ABCD2	0.018	0.833
TUSC5	0.03	0.883
ZNF831	0.005	0.859
CELF2	<0.001	0.800
CHL1	0.043	0.821
SCARA5	0.001	0.871
PLA2G2A	0.01	0.890

OS, overall survival.

Table S3 Differentially expression genes (DEGs) with significant RFS predictor in the high immune/stromal scores group

Gene	RFS	
	P value	HR
Immune score group		
CD226	0.032	0.922
CMKLR1	0.027	0.901
FCRL3	0.019	0.930
CXCR5	0.033	0.932
FABP4	0.017	0.936
FCRL1	0.015	0.930
FCRLA	0.048	0.933
CCL14	0.037	0.905
SIGLEC7	0.026	0.879
GVIN1	0.021	0.883
TCL1A	0.041	0.937
RELN	0.017	0.916
AQP9	0.037	0.897
FCER2	0.031	0.926
CD300LG	0.038	0.901
THEMIS	0.027	0.896
PRKCB	0.033	0.888
C10orf128	0.026	0.878
ADAMDEC1	0.01	0.893
SCARA5	0.04	0.916
CD37	0.019	0.839
EMR1	0.025	0.858
CNTN2	0.037	0.875
BTK	0.044	0.837
BLK	0.044	0.907
CCR2	0.033	0.847
NCF1	0.028	0.828
CLEC12A	0.032	0.858
RASGRP2	0.026	0.816
NELL2	0.022	0.861
CSF3R	0.02	0.818
SNX20	0.048	0.809
P2RY13	0.024	0.837
KMO	0.011	0.794
CD1C	0.03	0.852
PLA2G2A	0.007	0.904
NLRC4	0.047	0.779
CLEC10A	0.005	0.846
CD1E	0.019	0.814
CHIT1	0.021	0.884
C19ORF59	0.028	0.848
LILRA1	0.046	0.795
AMICA1	0.041	0.793
GRAP2	0.005	0.752
CCL23	0.013	0.824
P2RY14	0.009	0.749
LTB	0.013	0.768
CXCR2	0.021	0.824
CSF2RB	0.042	0.744
TIFAB	0.08	0.740
EMR3	0.035	0.776
CFP	0.015	0.720
CD1B	<0.001	0.712
Stromal score group		
ARHGAP28	0.011	0.928
P2RX7	0.07	0.920
COL1OA1	0.017	0.928
FCRL3	0.019	0.930
FCRLA	0.048	0.933
FMO1	0.04	0.888
AQP9	0.037	0.897
PRKCB	0.033	0.888
C10orf128	0.026	0.878
SCAR5	0.04	0.916
BCHE	0.027	0.853
CCR2	0.033	0.847
RGS18	0.046	0.844
AMH	0.001	1.149
PLA2G2A	0.007	0.904
CHIT1	0.021	0.884
CXCR2	0.021	0.824
EMR3	0.035	0.776

RFS, recurrence free survival.